New Cross-Coupled Filter Design Using Improved Hairpin Resonators

Sheng-Yuan Lee, *Student Member, IEEE,* and Chih-Ming Tsai, *Member, IEEE*

***Abstract*—Stepped-impedance resonators have been thoroughly studied in this paper. Two equations for odd- and even-mode resonance are derived from a new network model. The size and resonant frequencies of the resonator could then be designed based on these two equations. A new resonator-embedded cross-coupled filter, constructed by stepped-impedance hairpin resonators and miniaturized hairpin resonators, is presented. This new filter is very compact and has lower spurious response. A 0° feed structure, which adds two transmission zeros to the filter response, is also studied. The two zeros are so close to the passband that the selectivity and out-of-band rejection of the filter are significantly increased. The design has been verified by experiment results.**

***Index Terms*—Coupled transmission lines, transmission-line resonators, elliptic filters, microwave circuits.**

I. Introduction

IN MICROWAVE communication systems, small-size and high-performance filters are always needed to reduce the cost and enhance the system performance. They can be designed in many different ways and by using different materials. Among them, planar filters are particularly attractive because they are compact and easy to manufacture. Therefore, there has been much research conducted on planar filters and their components, i.e., planar resonators [1]–[9]. For example, hairpin resonators, stepped-impedance resonators, and miniaturized hairpin resonators are used to make filters more compact, and elliptic filters can be realized by introducing cross-coupled effects.

Since resonators are the basic components of a planar filter, it is necessary to select proper resonator types used in filter design. A conventional half-wavelength open-line resonator is always too large [1]. To reduce the circuit size, Cristal and Frankel [2] folded the open-line resonator to form a hairpin resonator. In 1989, the miniaturized hairpin resonator was developed by Sagawa *et al.* [5]. The coupled lines at the ends of this structure are used as a capacitor in order to reduce the resonator size. Therefore, this miniaturized hairpin resonator is much smaller than the hairpin resonator. Actually, this type of resonators is a variation of stepped-impedance resonators [4]. To begin this paper, many undiscovered important characteristics of this resonator will be discussed.

First of all, a new network model for miniaturized hairpin resonators is proposed. This new model accounts for all resonant modes. Two design equations are then derived based on this model. One of them is for the odd resonant modes and the other is for the even resonant modes. With some modification, these two equations can also be applied to similar resonators, such as stepped-impedance resonators and stepped-impedance hairpin resonators. A cross-coupled filter based on miniaturized hairpin resonators has been designed, fabricated, and measured to verify these equations. It is interesting to note that this new filter has an extra transmission zero, which can be adjusted for better rejection of interference signal without sacrificing the passband response.

Besides selecting resonator types, filter topology must also be considered carefully. Traditionally, parallel-coupled-line filters and hairpin filters are widely used in microwave circuits [1], [2]. They are constructed by identical resonators cascaded in series. With this topology, only Chebyshev and Butterworth responses can be realized. In order to enhance filter performance, cross-coupled filters, which can realize elliptic or quasi-elliptic response, were proposed in [3], [7], and [8]. In this paper, a new cross-coupled filter using resonator-embedded topology is presented. There are two types of resonators in this filter topology: the stepped-impedance hairpin and miniaturized hairpin resonators. They are specially arranged and designed to reduce the circuit size, create the cross-coupled effect, and lower the spurious response.

Finally, a 0° feed structure of a four-pole cross-coupled filter is studied. Compared with those filters designed with a 180° feed structure [7], [9], a filter with this new feed topology has two extra zeros near its passband. This makes the filter have steeper rejection. The new design has been verified by experiment results.

II. Resonant Conditions of Stepped-Impedance Resonators

Fig. 1(a) shows a typical miniaturized hairpin resonator and its parameters. The coupled-line section of this resonator can be modeled by an ideal transformer and two open stubs, as shown in Fig. 1(b) [10]. The turn ratio of the ideal transformer is $-1:1$. The characteristic impedance of open stub 1 is half of the odd-mode impedance of the coupled lines, and the impedance of open stub 2 is half of the even-mode impedance of the coupled lines.

When the circuit is excited at its odd modes, the fields are antisymmetrical. The voltage at point A is zero. In addition, the voltage at node 3 is equal to the negative of the voltage at node 4. The coupled-line section is excited at its own odd modes. Therefore, the circuit model can be split at point A with the

Manuscript received March 2, 2000; revised August 23, 2000. This work was supported in part by the National Science Council, Taiwan, R.O.C. under Grant NSC 88-2213-E006-076.

The authors are with the Department of Electrical Engineering, National Cheng Kung University, Tainan 70101, Taiwan, R.O.C.

Publisher Item Identifier S 0018-9480(00)10778-1.

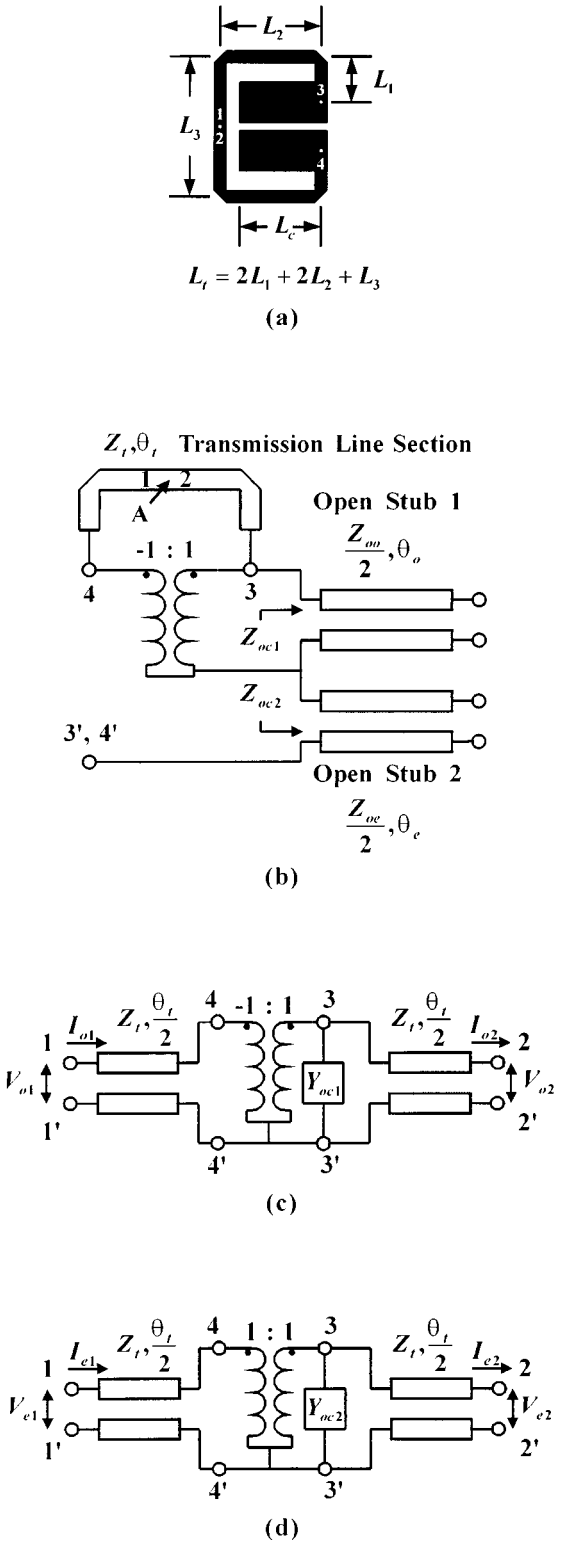

Fig. 1. (a) Miniaturized hairpin resonator. (b) Network model. (c) Odd-mode model. (d) Even-mode model.

conditions $I_{o1} = I_{o2}$ and $V_{o1} = V_{o2} = 0$, as shown in Fig. 1(c). The circuit can then be described by

$$\begin{bmatrix} V_{o1} \\ I_{o1} \end{bmatrix} = \begin{bmatrix} A_o & B_o \\ C_o & D_o \end{bmatrix} \begin{bmatrix} V_{o2} \\ I_{o2} \end{bmatrix} \tag{1}$$

with

$$\begin{bmatrix} A_o & B_o \\ C_o & D_o \end{bmatrix} = \begin{bmatrix} \cos\frac{\theta_t}{2} & jZ_t \sin\frac{\theta_t}{2} \\ jY_t \sin\frac{\theta_t}{2} & \cos\frac{\theta_t}{2} \end{bmatrix} \begin{bmatrix} -1 & 0 \\ 0 & -1 \end{bmatrix} \cdot \begin{bmatrix} 1 & 0 \\ Y_{oc1} & 1 \end{bmatrix} \begin{bmatrix} \cos\frac{\theta_t}{2} & jZ_t \sin\frac{\theta_t}{2} \\ jY_t \sin\frac{\theta_t}{2} & \cos\frac{\theta_t}{2} \end{bmatrix} \tag{2}$$

where $Y_{oc1} = 1/Z_{oc1} = 2j/Z_{oo} \cot\theta_o$. The equation for all odd-mode resonance, including the fundamental mode, can then be derived by using the conditions at point A, and the result is

$$\tan\frac{\theta_t}{2} = \frac{Z_{oo}}{Z_t} \cot\theta_o. \tag{3}$$

On the other hand, when the circuit is excited at its even modes, the fields are symmetrical. The circuit is open at point A. By similar reasoning, the even-mode circuit model can be derived, and is shown in Fig. 1(d) with the conditions $I_{e1} = I_{e2} = 0$ and $V_{e1} = V_{e2}$. The circuit is described by

$$\begin{bmatrix} V_{e1} \\ I_{e1} \end{bmatrix} = \begin{bmatrix} A_e & B_e \\ C_e & D_e \end{bmatrix} \begin{bmatrix} V_{e2} \\ I_{e2} \end{bmatrix} \tag{4}$$

with

$$\begin{bmatrix} A_e & B_e \\ C_e & D_e \end{bmatrix} = \begin{bmatrix} \cos\frac{\theta_t}{2} & jZ_t \sin\frac{\theta_t}{2} \\ jY_t \sin\frac{\theta_t}{2} & \cos\frac{\theta_t}{2} \end{bmatrix} \begin{bmatrix} 1 & 0 \\ 0 & 1 \end{bmatrix} \cdot \begin{bmatrix} 1 & 0 \\ Y_{oc2} & 1 \end{bmatrix} \begin{bmatrix} \cos\frac{\theta_t}{2} & jZ_t \sin\frac{\theta_t}{2} \\ jY_t \sin\frac{\theta_t}{2} & \cos\frac{\theta_t}{2} \end{bmatrix} \tag{5}$$

where $Y_{oc2} = 1/Z_{oc2} = 2j/Z_{oe} \cot\theta_e$. The equation for all even-mode resonance, including the first spurious mode, can then be derived, and the result is

$$\cot\frac{\theta_t}{2} = -\frac{Z_{oe}}{Z_t} \cot\theta_e. \tag{6}$$

It should be noted that the equation for "even"-mode resonance given by Sagawa [5] is not correct because it is derived based on the fundamental "odd"-mode condition of the stepped-impedance resonator given by Makimoto [4].

It is found that similar equations can also be applied to stepped-impedance resonators and stepped-impedance hairpin resonators. Fig. 2 shows the circuits and parameters of a typical stepped-impedance resonator and a stepped-impedance hairpin resonator. These two resonators can be treated as variations of the miniaturized hairpin resonators with an infinite or large space between the two conductors of the coupled lines. The coupled lines become two independent transmission lines and the center transmission-line section is unaffected. This makes $Z_t = Z_1$, $\theta_t = 2\theta_1$, $Z_{oo} = Z_{oe} = Z_2$, and $\theta_o = \theta_e = \theta_2$ in

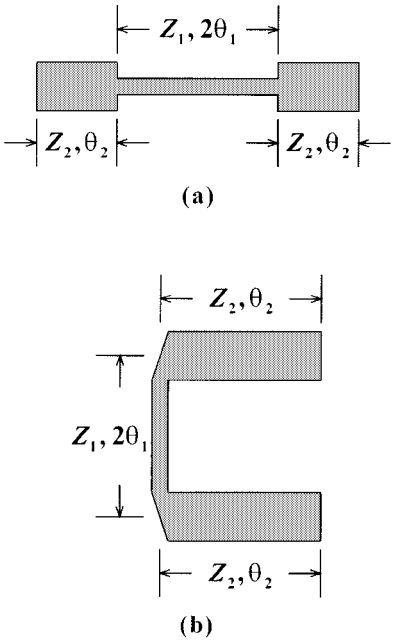

Fig. 2. (a) Stepped-impedance resonator. (b) Stepped-impedance hairpin resonator.

(3) and (6). The equations for these two resonators can then be written as

$$\tan\theta_1 = \frac{Z_2}{Z_1}\cot\theta_2 \tag{7}$$

and

$$\cot\theta_1 = -\frac{Z_2}{Z_1}\cot\theta_2 \tag{8}$$

where (7) is for the odd modes and (8) is for the even modes. Equation (7) is the same as the fundamental resonant equation given by [4], but (8) is different from the first higher order resonant equation in that paper. It is more general than Makimoto's equation, which is under the assumption of $\theta_1 = \theta_2$.

III. Characteristics of Miniaturized Hairpin Resonators

For miniaturized hairpin resonators, the fundamental mode is the first odd mode and the lowest spurious mode is the first even mode. Since they are very important in the design of filters, it is necessary to analyze the characteristics of these two modes. This analysis can also be applied to stepped-impedance resonators and stepped-impedance hairpin resonators, with the circuit parameters given in the previous section.

According to (3), Fig. 3 is plotted to illustrate the variation of the fundamental mode frequency due to the different impedance ratio of Z_{oo} to Z_t and the different length ratio of θ_o to θ_t. The total electrical length $\theta_t + 2\theta_o$ of these resonators are selected to be π at f_0. This makes the circuit resonate at f_0 when the impedance ratio is equal to one. It is clear that the smaller the impedance ratio of Z_{oo} to Z_t, the lower the fundamental resonant frequency. The resonant frequency is below or higher than f_0 when the impedance ratio is smaller or larger than one, respectively. For the impedance ratio less than one, it shows that the larger the length ratio, the lower the fundamental resonant

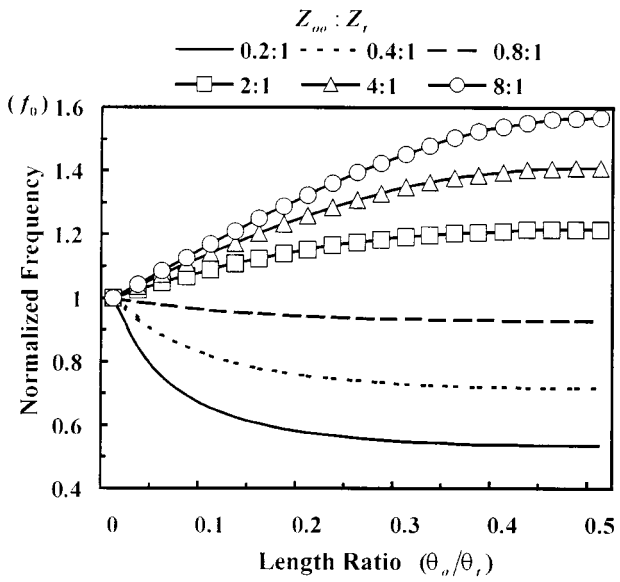

Fig. 3. Effects of impedance ratio of Z_{oo} to Z_t and length ratio of θ_o to θ_t on the fundamental-mode resonant frequency.

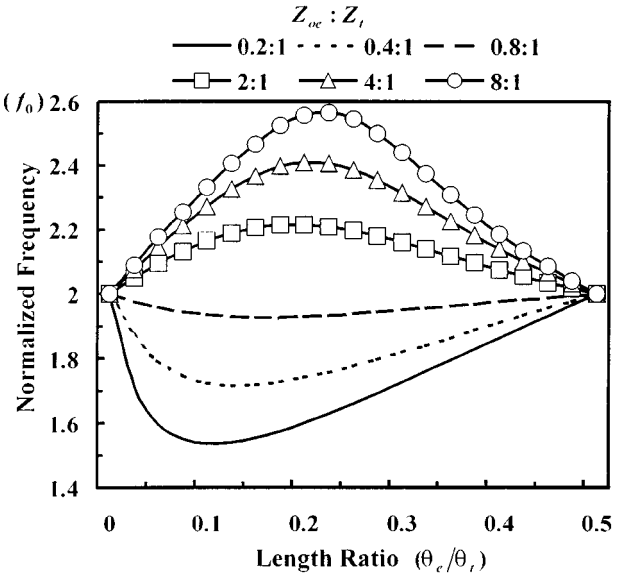

Fig. 4. Effects of impedance ratio of Z_{oe} to Z_t and length ratio of θ_e to θ_t on the first spurious-mode resonant frequency.

frequency. On the other hand, for the impedance ratio great than one, it shows that the larger the length ratio, the higher the fundamental resonant frequency. When the length ratio is equal to zero, a miniaturized hairpin resonator becomes a half-wavelength open-line resonator and the resonant frequency is fixed at f_0. Therefore, the impedance ratio should be as small as possible and the length ratio should be as large as possible when the size of the resonator has to be minimized.

Similarly, Fig. 4 is plotted according to (6) for the first spurious response of miniaturized hairpin resonators. The total electrical length $\theta_t + 2\theta_e$ of these resonators are also selected to be π at f_0. This makes the first spurious mode resonate at $2f_0$ when the impedance ratio of Z_{oe} to Z_t is equal to one. This figure shows the variation of the first spurious-mode frequency due

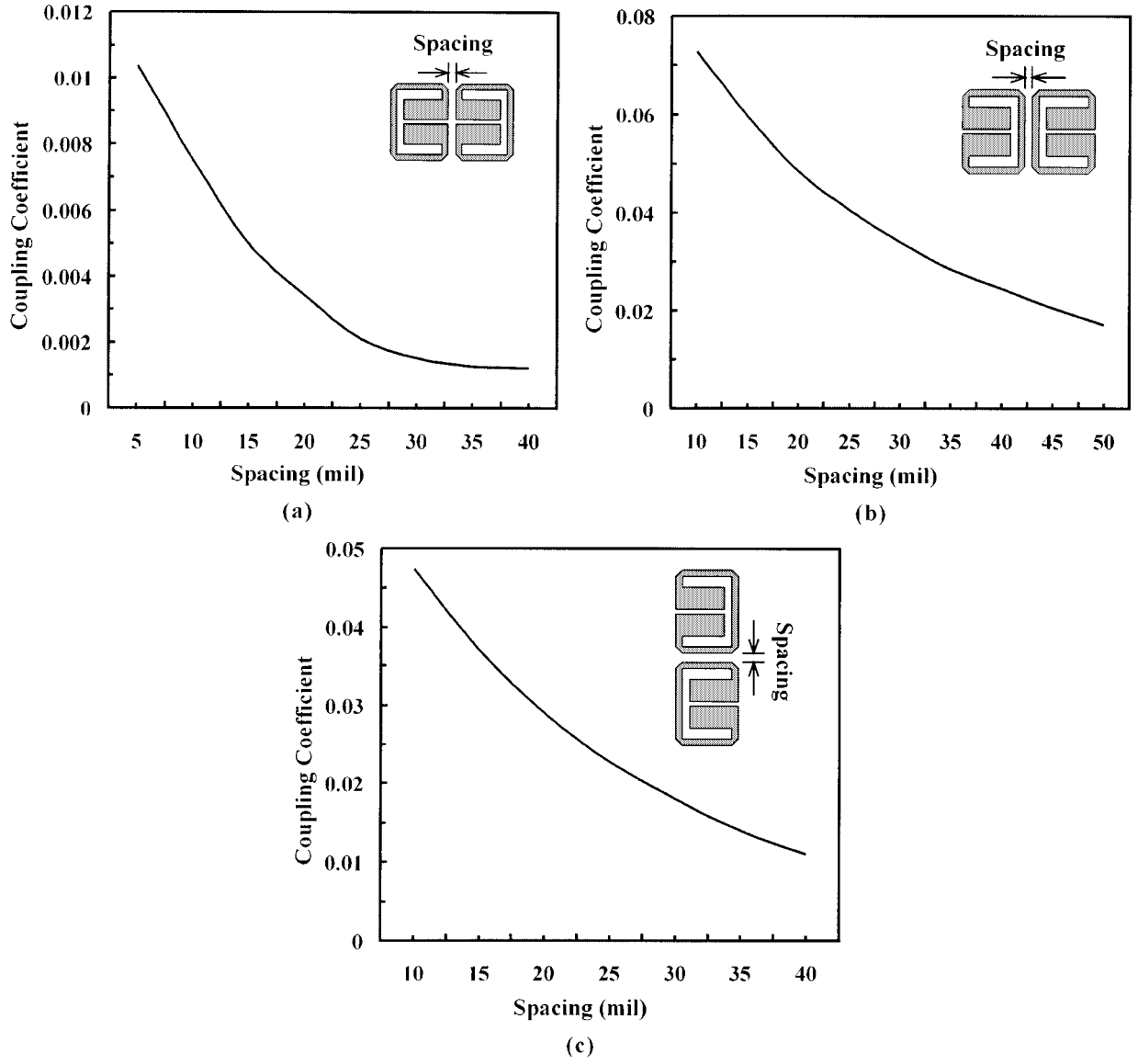

Fig. 5. Coupling structures and design curves for: (a) electric coupling, (b) magnetic coupling, and (c) mixed coupling.

to the different impedance ratio of Z_{oe} to Z_t and the different length ratio of θ_e to θ_t. It is clear that the larger the impedance ratio, the higher the first spurious-mode frequency. The resonant frequency is lower or higher than $2f_0$ when the impedance ratio is smaller or larger than one. For any impedance ratio smaller than one, the spurious frequency is lowest when the length ratio of a miniaturized hairpin resonator is about 0.14. On the other hand, for any impedance ratio larger than one, the spurious frequency is highest when the length ratio of a miniaturized hairpin resonator is about 0.21.

Therefore, properly selecting the values of Z_t, Z_{oo}, Z_{oe}, θ_t, θ_o, and θ_e is very important in the design of this type of resonators. The size can be greatly reduced and the first spurious-mode frequency could be properly designed.

IV. Four-Pole Cross-Coupled Filter Design

To demonstrate the applications of the studies in the previous section, a four-pole cross-coupled filter [3], [7] with center frequency f_0 at 2.0 GHz and 3.5% bandwidth was designed. The circuit was fabricated on the Rogers RO4003 substrate with a relative dielectric constant of 3.38, a loss tangent of 0.0027, and a thickness of 20 mil. In order to design a compact filter with a higher first spurious-mode frequency, the selected miniaturized hairpin resonator has the circuit parameters as

$$\begin{aligned} Z_t &= 65\ \Omega \\ Z_{oo} &= 25\ \Omega \\ Z_{oe} &= 31\ \Omega \\ L_t &= 1076\ \text{mil} \\ L_c &= 203.5\ \text{mil}. \end{aligned} \tag{9}$$

The resonator has the fundamental mode at 2.0 GHz and the first spurious mode at 4.7 GHz, which are calculated by using (3) and (6). Fig. 5 shows the three basic coupling structures and the design curves for this filter. The coupling structure in Fig. 5(a) is for electric coupling because the electric fringe fields

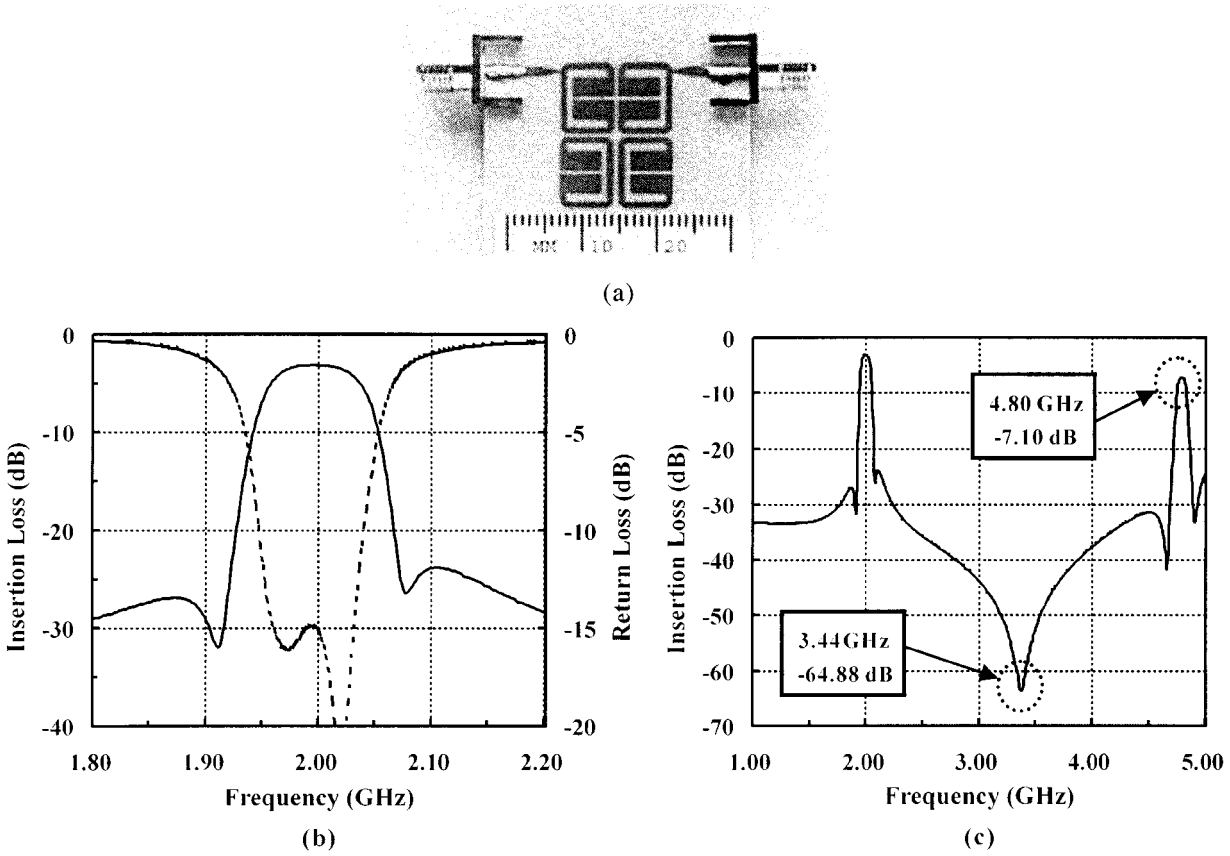

Fig. 6. (a) Four-pole cross-coupled filter. (b) Measured passband response. (c) Measured passband and spurious response.

are stronger near the open ends of the resonators. By similar reasoning, the structure in Fig. 5(b) provides a magnetic coupling because the magnetic fringe fields are stronger near the center of the resonators. The coupling structure in Fig. 5(c) provides both electric and magnetic coupling. The design curves in these figures are the results of electromagnetic analysis.

For the given specifications, the coupling coefficients and the loaded Q_{ext} of this filter can be found as

$$K = \begin{bmatrix} 0 & 0.023 & 0 & -0.0026 \\ 0.023 & 0 & 0.019 & 0 \\ 0 & 0.019 & 0 & 0.023 \\ -0.0026 & 0 & 0.023 & 0 \end{bmatrix} \quad (10)$$

$$Q_{\text{ext}} = 32.7.$$

Fig. 6(a) shows the photograph of the filter. The size of this filter amounts only to $0.167\lambda_0$ by $0.214\lambda_0$, where λ_0 is the guided wavelength on this substrate at the center frequency.

The filter was fabricated and measured using an HP 8719D network analyzer. Fig. 6(b) and (c) show the measured data. The passband insertion loss is about 2.8 dB. This is mainly due to the conductor and dielectric losses of the substrate. The passband return loss is no less than 15 dB. The out-of-band rejection is better than 27 dB at the lower stopband and 23 dB at the upper stopband. The filter has the center frequency f_0 at 2.0 GHz and the first spurious response at about 4.8 GHz. These justify the resonator design equations. It is interesting to notice that there is a 65-dB attenuation at 3.4 GHz. This is mainly due to the coupling of the slots in the filter layout. This should be useful in the rejection of strong interference in the stopband and can be fine tuned by changing the slot length without sacrificing the passband response.

V. Resonator-Embedded Four-Pole Cross-Coupled Filter Design

Traditionally, a planar bandpass filter is designed with several identical resonators. The circuit size is large and the spurious response is usually fixed at the double of the fundamental-mode frequency. Several types of resonators have been designed to overcome these problems such as stepped-impedance resonators, miniaturized hairpin resonators, and slow-wave open-loop resonators [4], [5], [9]. These resonators are used for reducing the filter size, but the spurious response of them are still large. Another method is to modify the filter structure to reduce the circuit size, such as the pseudointerdigital filter proposed by Hong and Lancaster [6]. However, the spurious response of this filter is fixed at the double of the fundamental-mode frequency. In this section, a new filter structure with embedded resonators is proposed. The circuit size is reduced, the spurious-mode frequency is controllable, and the level of the spurious response is lower.

Fig. 7(a) shows the topology of this new resonator-embedded four-pole cross-coupled filter. It is constructed by two types of resonators. One is the miniaturized hairpin resonator and the other is the stepped-impedance hairpin resonator. In order to reduce the filter size, the miniaturized hairpin resonators are em-

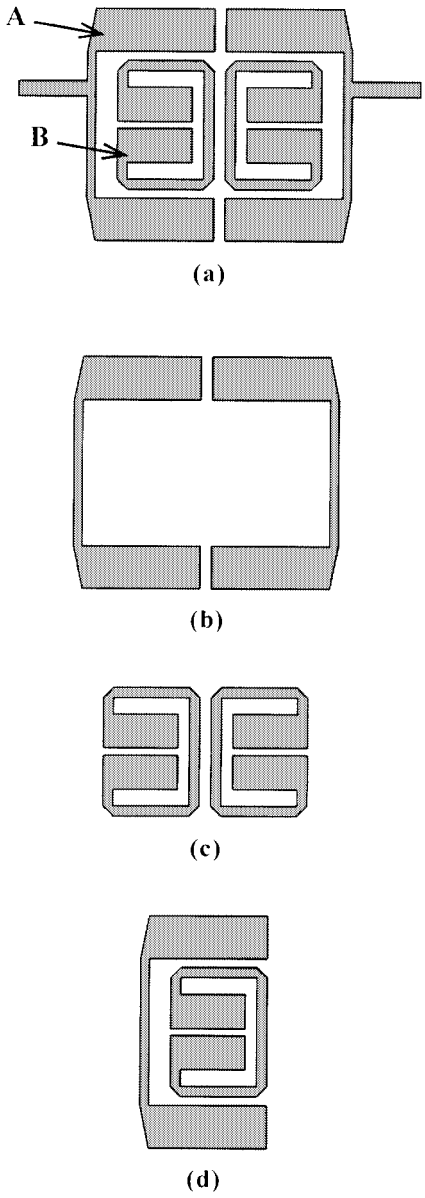

Fig. 7. (a) New resonator-embedded cross-coupled filter. (b) Electric coupling structure. (c) Magnetic coupling structure. (d) Mixed coupling structure.

bedded in the stepped-impedance hairpin resonators. This new filter has a fourth-order frequency response, but it is smaller than a hairpin-resonator filter with a second-order frequency response. Moreover, this special arrangement of resonators provides an additional signal path from the input resonator to the output resonator. This helps to create the cross-coupled effect. The frequency response of this filter could be elliptic or quasi-elliptic if properly designed. The first spurious-mode frequency can be predicted by using the equation derived in Section II. Since the miniaturized hairpin resonators are on the main signal path, the spurious-mode frequency will be dominated by the characteristics of these resonators. Another advantage of this new filter is that the level of the first spurious response is lower. This is because the first spurious-mode frequencies of these resonators are not the same. It is important to note that unwanted coupling effects in the stopband will increase when the center section of the resonator A is too close to the resonator B. Fortunately, this can be overcome by using the 0° feed structure, which will be discussed in the following section. Fig. 7(b)–(d) shows the three coupling structures encountered in this new filter. The coupling structure in Fig. 7(b) leads to an electric coupling and Fig. 7(c) leads to a magnetic coupling. Fig. 7(d) is similar to the mixed coupling structure in Fig. 5(c), except it is a dual-arm coupling structure. The coupling coefficient must be found by electromagnetic simulations.

A cross-coupled filter with this new resonator-embedded structure was designed with a center frequency at 2 GHz and 5% bandwidth. It was designed and fabricated on the Rogers RO4003 substrates. The parameters of the miniaturized hairpin resonators used in these structures are the same as those used in Section IV. The coupling coefficients and the loaded Q_{ext} of this filter is found as

$$K = \begin{bmatrix} 0 & 0.033 & 0 & -0.0037 \\ 0.033 & 0 & 0.028 & 0 \\ 0 & 0.028 & 0 & 0.033 \\ -0.0037 & 0 & 0.033 & 0 \end{bmatrix} \tag{11}$$

$$Q_{\text{ext}} = 22.8.$$

Fig. 8(a) shows the photograph of this filter. The size of this filter amounts only to $0.207\lambda_0$ by $0.182\lambda_0$, where λ_0 is the guided wavelength on this substrate at the center frequency.

The measured data is shown in Fig. 8(b) and (c). The passband insertion loss is about 2.4 dB and the passband return loss is greater than 15 dB. The out-of-band rejection is better than 30 dB. The filter has the center frequency f_0 at 2.01 GHz and the first spurious response at about 4.8 GHz. Its first spurious response is about 10 dB lower than the filter designed in Section IV.

VI. 0° Feed Structure

The input and output of a planar filter are usually achieved by tapped feed lines because they are simple and easy to design [11]. For a half-wavelength planer resonator, there are two proper feed points at the opposite locations about the center of the resonator. Fig. 9 shows two electric coupling structures constructed by hairpin resonators with different output feed points. In Fig. 9(a), the signals at the input and output feed points are in phase when the circuit is resonant at its fundamental-mode frequency, while in Fig. 9(b), they are out-of-phase. Both of these arrangements work, but the feed structure in Fig. 9(a) will create two more transmission zeros in the stopband. The first zero occurs at the frequency when the length of arm (2) of the input resonator approaches a quarter-wavelength and the other occurs at the frequency when the length of arm (1) is near a quarter-wavelength. To prove this, the equation for the insertion loss at these two frequencies are derived. When the length of arm (1) is a quarter-wavelength, the $ABCD$ matrices for the upper and lower signal path of the coupling structure in Fig. 9(a) can be derived as

$$\begin{bmatrix} A_u & B_u \\ C_u & D_u \end{bmatrix} = M_1 * M_2 * M_3 \tag{12}$$

and

$$\begin{bmatrix} A_l & B_l \\ C_l & D_l \end{bmatrix} = M_3 * M_2 * M_1 \tag{13}$$

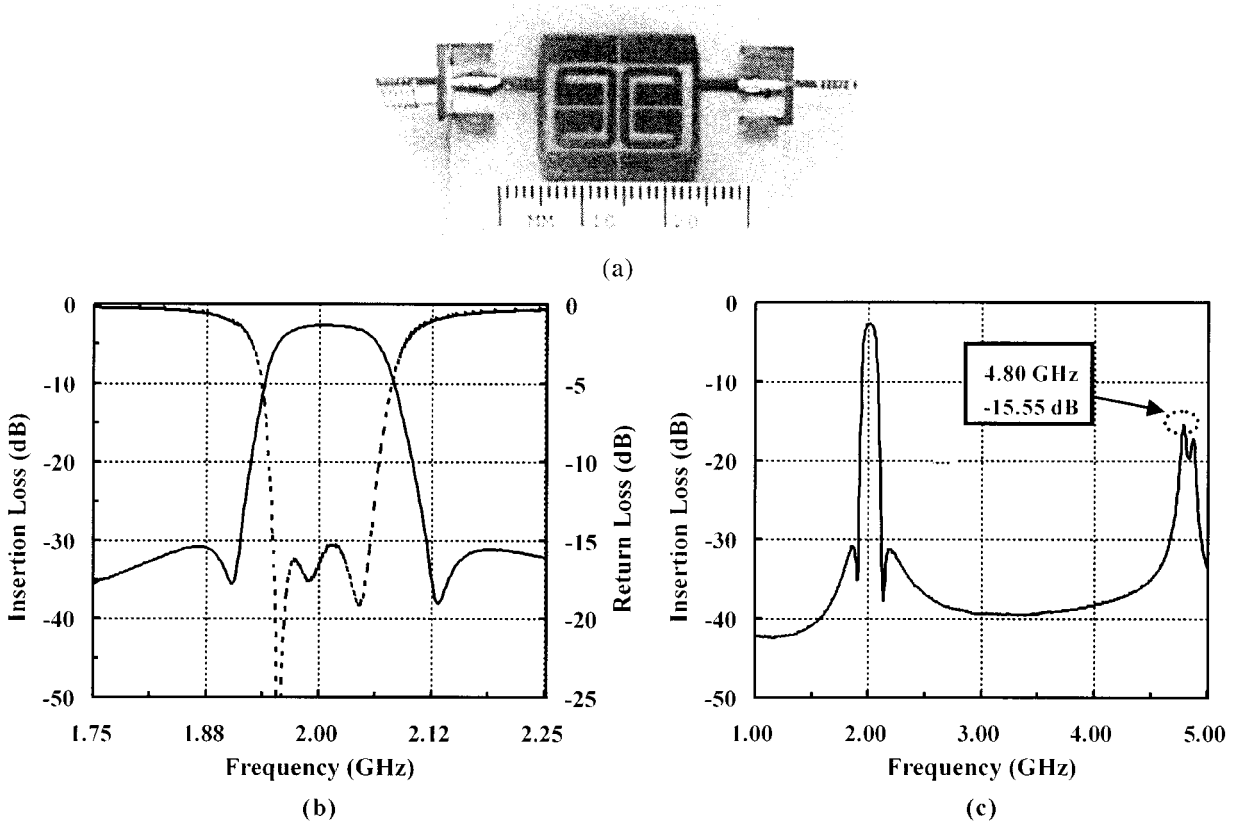

Fig. 8. (a)Resonator-embedded cross-coupled filter. (b) Measured passband response. (c) Measured passband and spurious response.

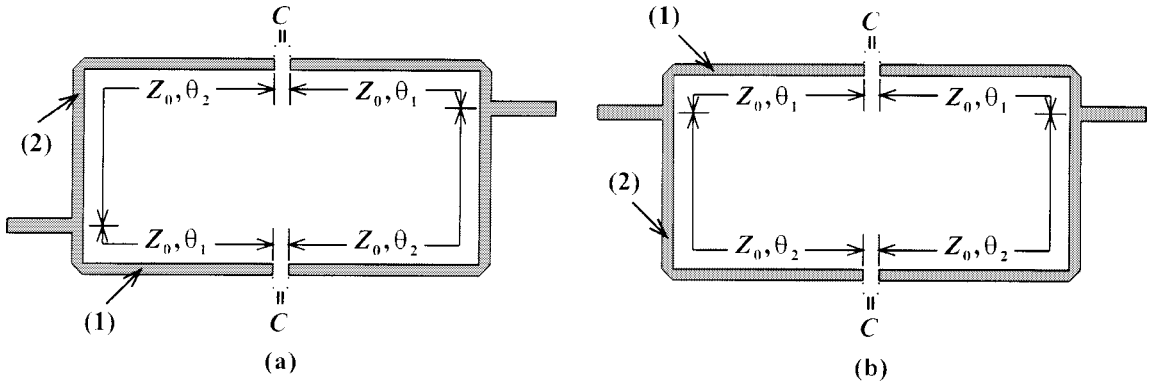

Fig. 9. Electric coupling structures of hairpin resonators with: (a) 0° feed structure and (b) 180° feed structure.

where

$$M_1 = \begin{bmatrix} \cos\theta_2 & jZ_0 \sin\theta_2 \\ jY_0 \sin\theta_2 & \cos\theta_2 \end{bmatrix} \quad M_2 = \begin{bmatrix} 1 & \frac{1}{j\omega C} \\ 0 & 1 \end{bmatrix}$$

and

$$M_3 = \begin{bmatrix} 0 & jZ_0 \\ jY_0 & 0 \end{bmatrix}$$

are the $ABCD$ matrices of the transmission-line arm (2), the mutual capacitor, and the transmission-line arm (1) in this coupling structure. The admittance matrix for each signal path is

$$\begin{bmatrix} Y_{11i} & Y_{12i} \\ Y_{21i} & Y_{22i} \end{bmatrix} = \begin{bmatrix} D_i/B_i & (B_iC_i - A_iD_i)/B_i \\ -1/B_i & A_i/B_i \end{bmatrix} \tag{14}$$

where $i = u$ or l for the upper or lower signal paths. The admittance matrix for the whole coupling structure is given by

$$\begin{bmatrix} Y_{11} & Y_{12} \\ Y_{21} & Y_{22} \end{bmatrix} = \begin{bmatrix} Y_{11u} & Y_{12u} \\ Y_{21u} & Y_{22u} \end{bmatrix} + \begin{bmatrix} Y_{11l} & Y_{12l} \\ Y_{21l} & Y_{22l} \end{bmatrix}. \tag{15}$$

The insertion loss can then be derived as

$$\begin{aligned} S_{21} &= \frac{-2Y_{21}Y_0}{(Y_{11}+Y_0)(Y_{22}+Y_0) - Y_{12}Y_{21}} \\ &= \frac{j4\cos\theta_2}{\left(\frac{Y_0}{\omega C}\cos\theta_2 - \sin\theta_2\right)^2 - 4}. \end{aligned} \tag{16}$$

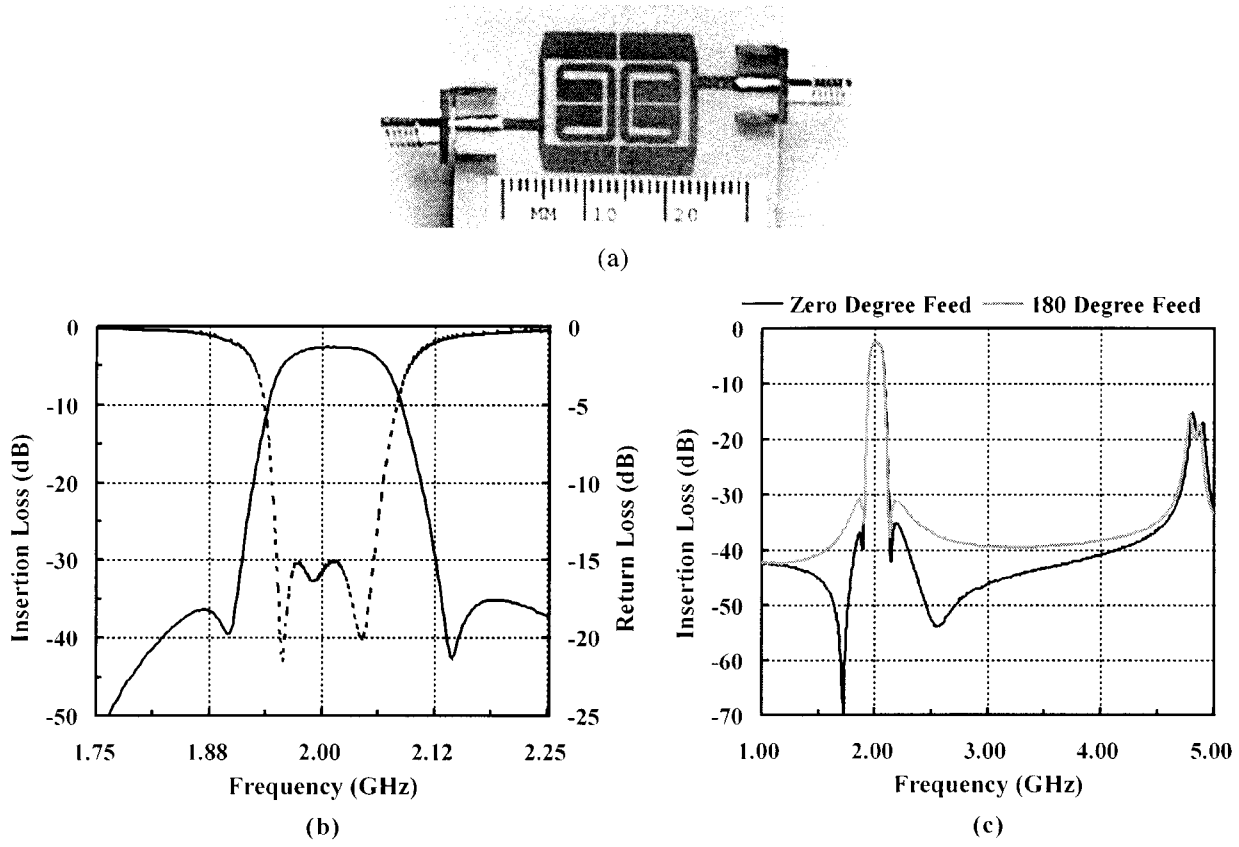

Fig. 10. (a) Resonator-embedded cross-coupled filter with zero-degree feed structure. (b) Measured passband response. (c) Measured passband and spurious response.

For an example, $f \cong 2$ GHz, $C \cong 0.01$ pF, $Y_0 \geq 0.01$ S, and $\theta_2 = 1.5\theta_1 = 1.5\pi/2$, this equation gives

$$S_{21} \cong \frac{j4}{\left(\frac{Y_0}{\omega C}\right)^2 \cos\theta_2} \leq j\Big(-8.93 \times 10^{-4}\Big). \tag{17}$$

Therefore, there is a deep attenuation (more than 60 dB) in the frequency response when θ_1 approaches $\pi/2$. This frequency is higher, but near the resonant frequency of the hairpin resonator because the length of arm (1) is a little bit shorter than the half-length of the hairpin resonator. With similar derivation, it can be shown that there is another deep attenuation in the frequency response when θ_2 approaches $\pi/2$. The frequency is lower, but also near the resonant frequency of the hairpin resonator. These two zeros are very helpful for out-of-band rejection because they are close to and on opposite sides of the passband. By similar reasoning, the electric coupling structures in miniaturized hairpin resonators or stepped-impedance hairpin resonators will also have similar response when 0° feed structure is used.

As mentioned previously, for a good out-of-band rejection, the resonator A in the new resonator-embedded filter should not be arranged too close to the resonator B. However, by using the 0° feed structure, these two resonators can now be placed closer without degrading the signal rejection level because the created two zeros can help to increase the rejection in the stopband.

A resonator-embedded cross-coupled filter with 0° feed structure was designed to verify the studies. This filter is the same as the filter design in Section V, except the feed structure. Fig. 10(a) shows the photograph of this filter. The measured data is given in Fig. 10(b) and (c). The passband insertion loss is about 2.4 dB and the passband return loss is greater than 15 dB. The out-of-band rejection is better than 35 dB. It is clear that the out-of-band rejection is increased. Compared to the filter design with a 180° feed structure, this filter has two extra transmission zeros at the stopband: one is at 1.72 GHz and the other is at 2.53 GHz. These two deeps are close to the passband and make the out-of-band rejection much better than the filter designed in Section V. The level of the first spurious response is also lower than the filter designed in Section IV.

VII. Conclusion

Two simple equations derived from a new network model for miniaturized hairpin resonator have been presented in this paper. These equations can also be applied to other types of stepped-impedance resonators. The resonant frequencies can be accurately predicted by using these equations. The impedance and length of the transmission lines and the coupled lines should be properly selected to minimize the circuit size and control the spurious response. A new resonator-embedded cross-coupled filter structure, constructed by stepped-impedance hairpin resonators and miniaturized hairpin resonators, has also been

presented. The circuit size of this new filter is smaller than the half-size of the same order direct-coupled planar filter. The level of the first spurious response is also lower than filters designed by using only one type of resonators. Finally, a 0° feed structure for four-pole cross-coupled filters has also been proposed. Filters with this type of feed structures can create two extra transmission zeros on opposite sides of the passband. The selectivity and out-of-band rejection of these filters are increased without any side effect on the passband response. Several filters using miniaturized hairpin resonators and stepped-impedance hairpin resonators has been designed, fabricated, and measured to verify the studies and demonstrate the applications. Among them, a traditional four-pole cross-coupled filter was designed. The results prove that the design equations for the miniaturized hairpin resonators are correct. Moreover, an adjustable transmission zero is found in the stopband. It is due to the coupling of the slots in the filter layout and could be useful for the rejection of interference signal in a communication system. Two other filters with different feed structures were designed by using the new resonator-embedded topology. The measured results again verify the design equations for the miniaturized hairpin resonators. The signal level of the first spurious response is also lower than common planar filters. These filters also indicate that the 0° feed structure can make a typical four-pole cross-coupled filter have higher selectivity and larger stopband rejection.

REFERENCES

[1] S. B. Cohn, "Parallel-coupled transmission-line-resonator filters," *IRE Trans. Microwave Theory Tech.*, vol. MTT-6, pp. 223–231, Apr. 1958.

[2] E. G. Cristal and S. Frankel, "Hairpin-line and hybrid hairpin-line/half-wave parallel-coupled-line filters," *IEEE Trans. Microwave Theory Tech.*, vol. MTT-20, pp. 719–728, Nov. 1972.

[3] R. Levy, "Filters with single transmission zeros at real or imaginary frequencies," *IEEE Trans. Microwave Theory Tech.*, vol. MTT-24, pp. 172–181, Apr. 1976.

[4] M. Makimoto and S. Yamashita, "Bandpass filters using parallel coupled stripline stepped impedance resonators," *IEEE Trans. Microwave Theory Tech.*, vol. MTT-28, pp. 1413–1417, Dec. 1980.

[5] M. Sagawa, K. Takahashi, and M. Makimoto, "Miniaturized hairpin resonator filters and their application to receiver front-end MIC's," *IEEE Trans. Microwave Theory Tech.*, vol. 37, pp. 1991–1997, Dec. 1989.

[6] J. S. Hong and M. J. Lancaster, "Development of new microstrip pseudo-interdigital bandpass filters," *IEEE Microwave Guided Wave Lett.*, vol. 5, pp. 261–263, Aug. 1995.

[7] ——, "Couplings of microstrip square open-loop resonators for cross-coupled planar microwave filters," *IEEE Trans. Microwave Theory Tech.*, vol. 44, pp. 2099–2109, Dec. 1996.

[8] M. Korber, "New microstrip bandpass filter topologies," *Microwave J.*, vol. 40, pp. 138–144, July 1997.

[9] J. S. Hong and M. J. Lancaster, "Theory and experiment of novel microstrip slow-wave open-loop resonator filters," *IEEE Trans. Microwave Theory Tech.*, vol. 45, pp. 2358–2365, Dec. 1997.

[10] C. M. Tsai and K. C. Gupta, "A generalized model for coupled lines and its applications to two-layer planar circuits," *IEEE Trans. Microwave Theory Tech.*, vol. 40, pp. 2190–2199, Dec. 1992.

[11] J. S. Wong, "Microstrip tapped-line filter design," *IEEE Trans. Microwave Theory Tech.*, vol. 27, pp. 44–50, Jan. 1979.

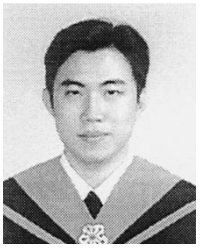

Sheng-Yuan Lee (S'96) was born in Taoyuan, Taiwan, R.O.C., on October 20, 1973. He received the B.S. degree in electronic engineering from the National Taiwan Institute of Technology, Taipei, Taiwan, R.O.C., in 1996, the M.S. degree in electrical engineering from the National Cheng Kung University, Tainan, Taiwan, R.O.C., in 1998, and is currently working toward the Ph.D. degree at the National Cheng Kung University.

His research interests include microwave planar filter design and passive circuit design.

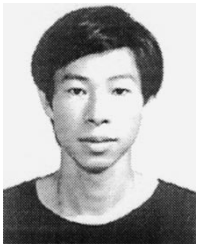

Chih-Ming Tsai (S'92–M'95) was born in Taipei, Taiwan, R.O.C., in 1965. He received the B.S. degree in electrical engineering from the National Tsing Hua University, Taiwan, R.O.C., in 1987, the M.S. degree in electrical engineering from the Polytechnic University, New York, NY, in 1991, and the Ph.D. degree in electrical engineering from University of Colorado at Boulder, in 1993.

From 1987 to 1989, he was a Member of Technical Staff on microwave communications at Microelectronic Technology Inc. In 1994, he joined the Department of Electrical Engineering, National Cheng Kung University, Taiwan, R.O.C., where he is currently an Associate Professor. His research interests include microwave passive components, transceivers, and measurements.